

## Molecular Beacon-Based MicroRNA Biosensor for Imaging EPC-Treated Cellular Therapy of Ischemia

Chang Hyun Lee<sup>1</sup>, Jung il Chae<sup>2</sup>, Hae Young Ko<sup>1</sup> and Soonhag Kim<sup>1\*</sup>

<sup>1</sup>Department of Biomedical Science, CHA University, Seoul, Republic of Korea

<sup>2</sup>Department of Oral Pharmacology, School of Dentistry and Institute of Oral Bioscience, Chonbuk National University, Jeonju, Republic of Korea

### Abstract

Angiogenesis, the process of new blood vessel formation, is an important therapeutic target in cardiovascular and malignant diseases for diverse reasons. Molecular imaging for angiogenesis has been attracted due to the use of anti-angiogenic therapeutic drugs to treat tumours, and of therapeutic angiogenesis induction to treat vascular diseases. We developed a novel biosensor of imaging microRNA126 (mir126) expressed during angiogenesis using a miRNA Molecular Beacon (MB) composed of a stem loop-structured DNA complementary to mir126 and Cy5.5 (near infrared, NIR)-black hole quencher 2 (BHQ2) (mir126 NIR MB). Mir126 in cord blood-derived endothelial precursor cells (CB-EPCs) was highly expressed and more expressed after the wound healing. The quantitative and qualitative fluorescence intensity of the mir126 NIR MB was high in CB-EPC and significantly increased after the wound healing, showing a great specificity of sensing endogenous mir126. From the CB-EPC-treated hind limb ischemia, cellular morphology and immune histochemical analysis using antibodies of vWF and CD31 showed a successful induction of angiogenesis and vascularisation and fluorescence signals of the mir126 NIR MB was gradually increased during 6 days of the cellular therapy and much stronger than the signals of laser Doppler imaging. The mir126 NIR MB demonstrated that the mir126 sensor will be useful for early diagnosis of cellular therapy of ischemia and non-invasively sensitive imaging for cellular developments, diagnosis of disease and cellular therapy related to the miRNA function.

**Keywords:** MicroRNA; Biosensor; Molecular imaging; Molecular beacon; Angiogenesis; EPC

### Introduction

Angiogenesis are basic processes of new blood vessels formation. Vasculogenesis entails the differentiation of mesodermal cells into endothelial precursor cells. When vascular damage is occurred, vessels are able to regenerate via angiogenesis, which is formation of blood vessel from pre-existing blood vessel by the sprouting, splitting, and remodeling of the vascular network. Since the discovery of endothelial precursor cells (EPCs) has been believed that vasculogenesis be able to occur in adult, they have used for the application of cell therapy using putative endothelial cell population for several vascular diseases [1-3]. With this cell therapy concept several kinds of cellular sources which obtained from adult source were highlighted as stem cell reservoir, including cord blood, peripheral blood, fat, bone marrow, liver, and etc. Among them, cord blood is considered as valuable cellular source for vascular lineage cell obtaining due to their convenience, such as non-invasive acquisition procedure and enriched stem cell population in cord blood [4-6]. MicroRNAs (miRNAs) represent a class of about 22 nucleotide long, non-coding RNAs that have been recognized in the recent years as an important regulators of gene expression [7-9]. Predominantly, miRNAs repress protein expression by inhibiting target mRNA translation [10,11]. It is well-known that miRNAs functions are associated with a wide variety of cellular activities including fat metabolism, apoptosis, cellular differentiation and proliferation as well as clinically important diseases [9-18]. In an attempt to identify miRNAs involved in the control of endothelial cell function, three studies have profiled the expression of miRNAs (miR17-92 cluster, let7f, miR222, mir126) in endothelial cells [19-22]. Expanding evidence indicates the importance of miRNAs in blood vessel formation by the regulation of endothelial and smooth muscle cell functions [23,24]. By miRNA profiling of ES cell-derived endothelial cells, Fish et al. showed that mir126 identified a group of endothelial-enriched miRNAs. These miRNAs were also enriched in endothelial cells of developing mouse

embryos [22]. Recent investigations have revealed that the endothelial mir126 promotes angiogenesis. The mir126 regulates angiogenic activity of endothelial cell in response to angiogenic factors such as vascular endothelial growth factor (VEGF), Sprouty-related protein-1 (Sprd-1), vascular cell adhesion molecule-1 (VCAM-1) and basic fibroblast growth factor (bFGF) through targeting multiple proteins that modulate angiogenesis and vascular integrity [25]. In mice, targeted deletion or disruption of mir126 caused a loss of vascular integrity, which resulted in poor vessels development, eventually leading to embryonic lethality. Currently, mir126 is the only miRNAs known to be specifically expressed in the endothelial cell lineage and hematopoietic progenitor cells [22,25-27]. This suggests that mir126 is most important for maintaining vascular integrity during ongoing angiogenesis.

Recent technological development in molecular imaging, which has played a critical role in preclinical research to monitor noninvasively cellular therapy of cancer and a variety of biological processes including carcinogenesis, myogenesis, neurogenesis and angiogenesis, have provided fundamental improvements in understanding *in vivo* molecular mechanisms by various imaging modalities [28]. Most of molecular imaging reporter probes for diseases and cellular developments have been focused on targeting cellular membrane proteins or receptors,

**\*Corresponding author:** Soonhag Kim, Laboratory of Molecular Imaging, Department of Biomedical Science, CHA University, 605-21 Yoeksam 1-dong, Gangnam-gu, Seoul, Korea, Tel: +82-2-555-5063; Fax: +82-2-3468-3373, E-mail: [kimsoonhag@empal.com](mailto:kimsoonhag@empal.com)

**Received** June 19, 2013; **Accepted** August 06, 2013; **Published** August 10, 2013

**Citation:** Lee CH, Chae JI, Ko HY, Kim S (2013) Molecular Beacon-Based MicroRNA Biosensor for Imaging EPC-Treated Cellular Therapy of Ischemia. J Mol Imaging Dynam 2: 113. doi:10.4172/2155-9937.1000113

**Copyright:** © 2013 Lee CH, et al. This is an open-access article distributed under the terms of the Creative Commons Attribution License, which permits unrestricted use, distribution, and reproduction in any medium, provided the original author and source are credited.

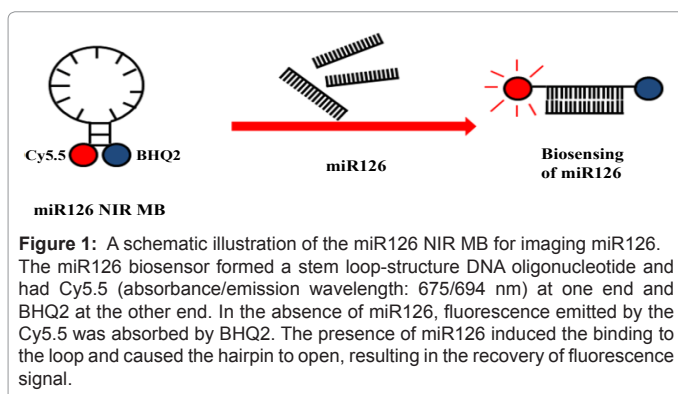
which ligands are solely dependent on the binding affinity of the ligands with their targets at the exterior boundary of the cells. These current methods are not applicable for imaging intracellular targets including miRNAs due to the placement of the probes in cells with or without interaction with their targets. Besides, most of the current methods to detect the expression of intracellularly expressed miRNAs are northern blot analysis, microarray and quantitative real-time polymerase chain reaction (qRT-PCR) which are invasive and only investigate a predefined two-dimensional plane [29,30]. Our recent developments of optical miRNA bio-sensors for imaging intracellularly expressed miRNAs using the bioluminescent reporter gene and fluorescent molecular beacon have successfully demonstrated *in vivo* imaging of miRNA-involved cellular developments including myogenesis, carcinogenesis and neurogenesis [29,31-35]. However, the bioluminescent miRNAs reporter gene represents signal-off system in the presence of miRNAs due to the miRNAs function that destabilizes transcriptional activity of its target mRNA. The decreased bioluminescent signals from this signal-off miRNAs imaging system are frequently challengeable to differentiate that from cellular loss. In addition, although the fluorescence miRNAs molecular beacon have successfully represented signal-on system in response to miRNAs expression, fluorescence dyes in the miRNA MB that have been used have short emission wavelength of the dye molecules which cause a limitation to acquire high quality *in vivo* image due to the high autofluorescence and low depth penetration. So the application of near-infrared (NIR) fluorescence dyes (670-900 nm wavelengths) into the miRNAs molecular beacon will be used an alternative for *in vivo* signal-on miRNAs imaging system, which can provide high imaging sensitivity from target tissues.

In this study, we developed a novel miRNAs biosensor to detect mir126 intracellularly expressed during the angiogenesis of EPC-treated ischemia using NIR-based miRNA MB (miR NIR MB). The mir126 NIR MB contained a synthetic stem loop-structured (hairpin) DNA oligonucleotide that bound to the mir126 and that had a Cy5.5 (excitation/emission, 675/694 nm) reporter fluorophore at one end and a nonfluorescent black hole quencher 2 (BHQ2) at the other end (Figure 1). In the absence of mir126, fluorescence signals of the mir126 NIR MB were quenched by the BHQ2 as a result of fluorescence resonance energy transfer (FRET). However, in the presence of mir126, the mir126 NIR MB underwent a spontaneous fluorogenic conformational change upon hybridization of mir126 to the complementary nucleic acid target within the loop of the mir126 NIR MB, resulting in the separation of Cy5.5 from the BHQ2 and recover fluorescence signals.

## Material and Methods

### Isolation of mononuclear cell population from cord blood

To derive cord blood-derived EPC (CB-EPCs), human umbilical



cord blood (45 ml) was collected-tubes from healthy volunteers from the CHA general hospital. After dilution of cord blood with D-PBS (Invitrogen, Carlsbad, CA) into 1:3 ratio, Ficoll-Paque (Amersham, Piscataway, NJ) was overloaded onto diluted cord blood, then centrifugation was performed at 2500 rpm for 30 minutes. Buffy coat mononuclear cells (MNCs) were collected and washed three times using D-PBS. MNCs were re-suspended in EGM-2-MV medium (Lonza, GA) supplemented with hEGF, hydrocortisone, GA-100, FBS (5%), VEGF, hFGF-B, R3-IGF-1 and ascorbic acid. Cells were seeded on Fibronectin-coated culture dishes. After five days of culture, non-adherent cells and debris were aspirated, and fresh EGM-2-MV culture medium was added. The research was approved by the Korea Ministry of Health and Welfare (National Approval Number 86) by the Act of Bioethics Law. According to this national approval, we were approved for the use of cord blood by the IRB of CHA University. HUVECs (human umbilical vascular endothelial cells) were purchase form Cambrex and cultured in EGM-2 medium (Lonza, GA).

### RT-PCR analysis

Total RNA from HUVEC and CB-EPC cells was isolated using the Trizol reagent (Invitrogen, CA). Reverse transcription was performed at 45°C for 60 minutes to synthesize the first-strand cDNA according to the manufacturer's instructions (maxime RT premix, Intron). Standard PCR conditions using a pair of primer for each gene (Supplementary Table 1) included 2 minutes at 95°C, followed by 20~28 cycles of 30 seconds of denaturing at 95°C, then 30 seconds of annealing at 55°C and 1 minute of extension at 72°C.

### Quantification of mir126 expression

Expression of mir126 from HeLa (human cervical cancer cell line, ATCC), human mesenchymal stem cells (MSC, kindly provided by Dr. Dongyeon Hwang in CHA University) and CB-EPCs were quantified by real-time reverse transcription (qRT-PCR) using total RNA. Real-time PCR of mature mir126 was conducted using the mirVana™ qRT-PCR primer Set and the mirVana™ qRT-PCR miRNA kit (both from Ambion). PCRs were performed in triplicate using an iCycler (Bio-Rad) and SYBR Premix Ex Taq (Takara, Japan) at 95°C for 3 min and 40 cycles of 95°C for 15 s and 60°C for 30 s. The relative amounts of each mature miRNA were normalized versus the U6 snRNA primer set (Ambion) using the equation  $2^{-\Delta\Delta CT}$ , where  $\Delta CT = (CT_{miRNA} - CT_{U6RNA})$ ,  $\Delta\Delta CT = (\Delta CT - \Delta CT_{miRNA \text{ of HT-or13}})$ . Data were expressed as mean and standard deviation of relative values obtained from three different samples. T-test was performed with significant p-value of 0.05 for comparison.

### Cell surface marker analysis

The expression of cellular surface biomarkers for endothelial cells, CB-EPCs and HUVEC, was determined by flow cytometry. Cells were dissociated with 0.25% Trypsin-EDTA (GIBCO, Grand Island, NY) and then washed with FACS buffer (PBS containing 2% FBS). They were incubated with either unstained control or antigen-specific antibodies for 20 min, including CD34-PE (BD Pharmingen), CD133 (Santa Cruz Biotechnology), KDR-PE (R&D Systems, MN), CD 31-PE (R&D Systems) and Tie-2-PE (R&D Systems, MN). Cells were washed twice in PBS containing 2% fetal bovine serum and resuspended in FACS buffer. FACS analysis was performed using a FACS Caliber Flow Cytometer (BD Bioscience, CA).

### Immunocytochemistry

Cells were fixed in 4% paraformaldehyde for 30 minutes and permeabilized with 0.1% Triton X-100 in PBS for 5 minutes. After

blocking with 3% bovine serum albumin for 1 hour, then were incubated overnight with primary antibodies at 4°C. Commercial antibodies used for Immunocytochemistry included vWF (1:700; Millipore, MA) and CD 31 (1:500; Millipore, MA). After being washed with PBS, the cells were incubated with secondary antibodies conjugated with Alexa 488 and Alexa 594 (Molecular Probes, NY) and visualized via confocal microscopy (LSM510; Zeiss) after counter-staining with 2 g/ml DAPI (Sigma, MO).

### Matrigel assays of tubule formation

To induce tubule formation, CB-EPCs and HUVECs were seeded onto six-well tissue culture plates coated with Matrigel (BD Biosciences, CA) at a cell density of  $2 \times 10^5$  cells per well. Cells were observed after 24 hours by an inverted microscope at 40X magnification in order to view capillary-like formations.

### Design of the mir126 NIR MB

Of several miRNAs highly expressed in angiogenic differentiation of CB-EPCs, mir126 was tested in the study. The mature mir126, mir126 antagomir and the mir126 NIR MB were purchased from Bionics (BIONICS, Seoul, Korea). The sequences of miRNAs are as follows: mir126 (5'-UUCAAGUAAUCCAGGAUA GGCU-3'). The sequences and the structure of the mir126 NIR MB were 5'-Cy5.5-TCGTACGCATTATTACTCACGGTACGA-BHQ2-3'.

### Fluorescence intensity

HeLa, MSC and CB-EPC cells were seeded onto a 24 well plate to the amount of  $2 \times 10^4$  cells in each well. After 24 hr, for imaging specificity of mir126 in MSC and HeLa cells, 50 pmol of the mir126NIR MB with either various concentrations (0, 5, 10 and 20 pmol) of exogenous mir126 or mir126 antagomir were transfected to HeLa and MSC cells. For imaging endogenous mir126, various concentrations (0, 1, 5, 20, 50 pmol) of the mir126 NIR MB were transfected into CB-EPC. Transfection was performed with Lipofectamine reagent (Invitrogen, CA). For each well, 2  $\mu$ l of Plus reagent and 8  $\mu$ l of Lipofectamine were used. After transfection for 3.5 h at 37°C, fluorescence intensity was measured using BioTek fluorescent microplate Fluorometer (Synergy MX, Biotek Ltd, VT), with 683 nm of excitation and 705 nm of emission.

### Wound healing migration assay

A culture plate where CB-EPCs were grown to confluence was scraped in a straight line to create a wound with a pipette tip. Both wound edges were marked with dotted white lines in (Figure 4b). Thereafter, the cells were washed with PBS to remove any debris and to smooth the edges of the wound prior to incubation for a period of 12 h at 37°C in endothelial differentiation media. The mir126 NIR MB was transfected into the wound-healed CB-EPCs using Lipofectamine 24 hr before the wound healing. The fluorescence images were acquired 28 hr after the wound healing.

### In vivo imaging of CB-EPCs treated cellular therapy of ischemia

All mice were housed in specific pathogen-free conditions and were carried out in accordance with the institutional animal care and use committee in CHA University. After 7-week-old male ICR mice (Japan SLC, Shizuoka, Japan) were anesthetized with pentobarbital (80 mg/kg, i.p.), hindlimb ischemia was induced by the ligation of the right femoral artery including the superficial and the deep branch with 7-0 silk suture and the wound was closed using surgical staples. To treat the hindlimb ischemia,  $2 \times 10^6$  of HeLa (as a negative control) and CB-EPC cells were mixed in 150  $\mu$ l of PBS and resuspended within 150  $\mu$ l of

Matrigel (BD Bioscience, CA) on ice. Before closing the wound, these cells were transplanted on the top of the surgical operation site where the right femoral artery was ligated. The measurement of hind limb blood flow was performed with a LDPI analyzer (Moor Instruments, Devon, United Kingdom) and AV. *In vivo* imaging of the mir126 NIR MB from the cells-treated ischemia was acquired using the IVIS<sup>®</sup> spectrum imaging system (Caliper Life Sciences, MA) for 6 days.

### Immunohistochemistry and hematoxylin and eosin (H&E) staining

HeLa cells- or CB-EPC-incorporated matrigel in the hind limb ischemia was isolated, embedded in paraffin, sectioned, and analyzed by immunohistochemistry (IHC) 6 days after from transplantation. Paraffin sections were blocked with mouse-on mouse reagent (Vector Laboratories). A mouse anti-human CD31 antibody (1:200 dilution) and a rabbit anti-human vWF polyclonal antibody (1:200 dilution) were stained with its corresponding secondary antibody conjugated with Alexa 488 and Alexa 594 (Molecular Probes, NY) and visualized by a confocal microscopy (LSM510; Zeiss) after counter-staining with 2 g/ml DAPI (Sigma Aldrich, MO). For the H&E staining, 7  $\mu$ m-thick sections were deparaffinized in xylene and hydrated through sequential ethanol gradient. H&E images were captured with Nikon fluorescence microscope (Nikon, Japan).

### Statistical analysis

All data are presented as the means  $\pm$  SD calculated from quadruple wells and significant differences between samples were assessed using a Student's t-test (\* $P < 0.05$ ).

## Results

### Specificity of the mir126 NIR MB for sensing of mir126

To sense mir126 expression using the mir126 NIR MB, we first investigated the expression of miRNA<sub>126</sub> in various cell lines mesenchymal stem cells (MSCs), CB-EPCs and HeLa cells (cervical cancer cells) by real-time PCR for mature miRNA<sub>126</sub>. Similar to other reports [36], CB-EPCs cells showed relatively high expression of miRNA<sub>126</sub> while MSC and HeLa cells showed little expression of mir126 (Figure 2A). To study the biosensing specificity of imaging mir126, the mir126 NIR MB was first tested in solution with various concentrations (0, 5, 10, 20, 50 and 100 pmol) of exogenous mir126 in microtube (Figure 2B). The fluorescence intensity of the mir126 NIR MB was gradually increased in a dose dependent manner, while it remained at the original quenched status after the treatment (100 pmol) of a mir126 antagomir that is a synthetic oligonucleotide that fully complements the nucleotide sequences of mir126. To further determine the signal-on specificity of sensing mir126 in cells, the mir126 NIR MB was co-transfected with the exogenous mir126 into HeLa cells and MSCs where the endogenous expression of mir126 was little. The mir126 NIR MB was quenched in both cells with the treatment of 0 pmol of the exogenous miRNA<sub>126</sub> or 20 pmol of the mir126 antagomir while the quantitative fluorescence intensities of the mir126 NIR MB were significantly and gradually increased with the addition of various concentrations (5, 10 and 20 pmol) of the exogenous mir126 (Figure 2C). Similarly, confocal microscopy imaging with treatment of exogenous mir126 showed a gradual fluorescence brightness in the cytoplasm of both HeLa cells and MSCs transfected with the mir126 NIR MB (Figure 2D). However, no clear fluorescence signal was visualized with the treatment of mir126 antagomir from both cells containing the mir126 NIR MB. These results suggested that the complementary oligonucleotide sequences in the stem loop of the mir126 NIR MB was specifically bound by mir126 and

resulted in fluorescence recovery from the mir126 NIR MB, implying a great specificity of sensing mir126 expression.

### Characterization and comparison of CB-EPCs and HUVECs

To image cellular therapy of EPC-treated ischemia, isolation of CB-EPCs and HUVECs were derived from mononuclear cell fraction of

cord blood by ficoll density gradient method and human umbilical cord by enzyme treatment. The morphological analysis of both CB-EPCs and HUVECs showed representative endothelial cell cobblestone-like morphology in culture (Supplementary Figure 1A). RT-PCR analysis demonstrated that the transcriptional expression of endothelial cell specific genes, including KDR (Kinase domain receptor, known as

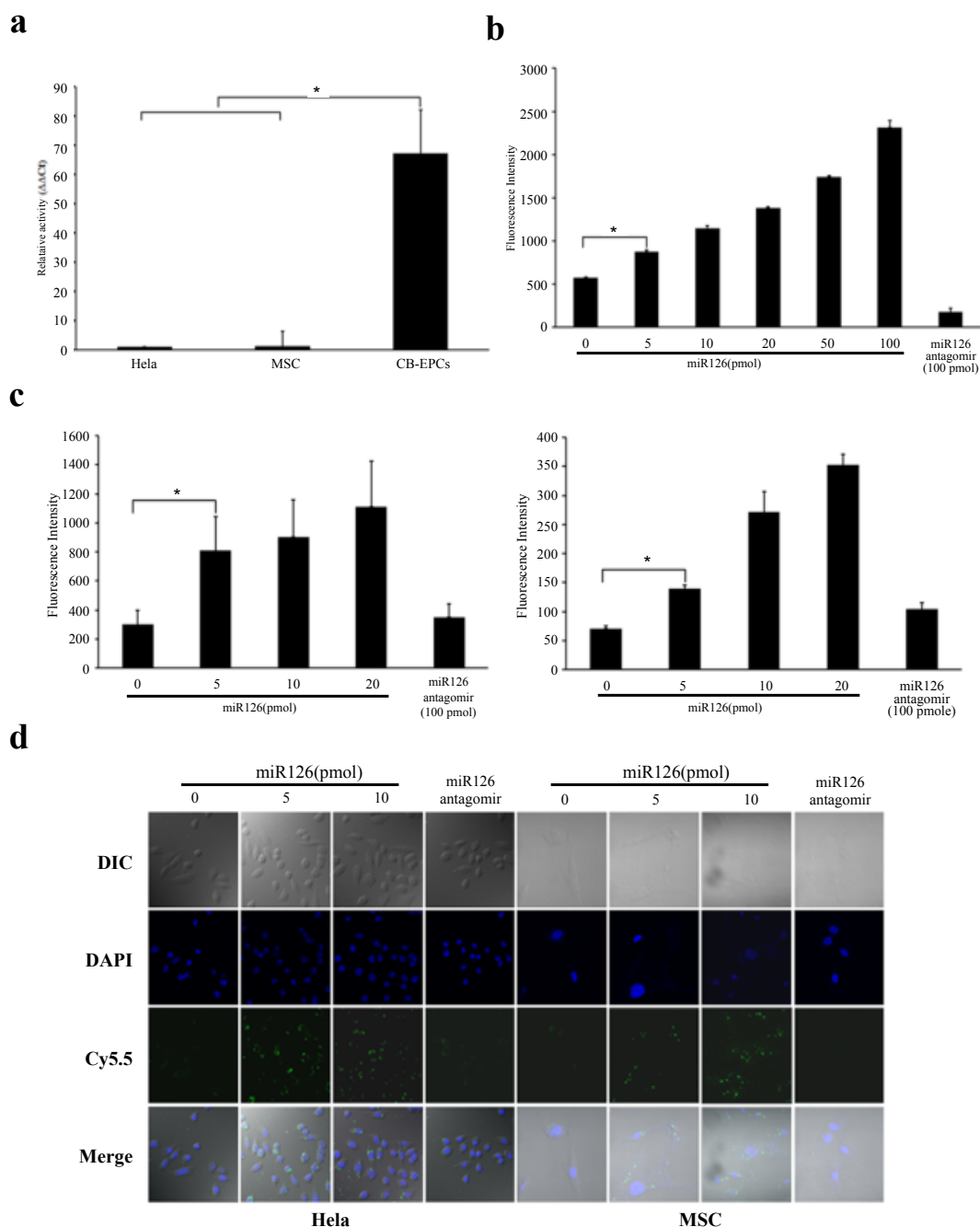


**Figure 2:** Specificity of sensing miR126 by the miR126 NIR MB.

a) Real time PCR for mature miR126 in HeLa, MSC and CB-EPCs. b) Quantitative fluorescence analysis of the miR126 NIR MB in microtube. Various concentrations (0, 5, 10, 20, 50 and 100 pmol) of miR126 or 100 pmol of miR126 antagonist were incubated with 50 pmol of the miR126 NIR MB. Fluorescence intensity of the miR126 NIR MB showed a positive correlation with the dose of miR126. c) Fluorescence analysis of the miR126 NIR MB in HeLa (left panel) and MSC (right panel) cells. Various concentrations (0, 5, 10 and 20) of miR126 or 100 pmol of miR126 antagonist were co-transfected into HeLa and MSCs with 50 pmol of the miR126 NIR MB. (a-c) All data were displayed as mean  $\pm$  standard error (\* $P$ <0.05). d) Confocal microscopy analysis (X400) of the miR126 NIR MB in HeLa and MSC cells. Various concentrations (0, 5 and 10 pmol) of miR126 or 100 pmol of miR126 antagonist were co-transfected into HeLa and MSCs with 50 pmol of the miR126 NIR MB. Fluorescence image was acquired at excitation of 675 nm and emission of 694 nm. All figures are merged with the 4', 6-diamidino-2-phenylindole (DAPI) image (nucleus staining, 460 nm) and cellular morphology. 10 pmol of miR126 NIR MB was transfected into HeLa cells.

VEGF receptor-2), vWF (Von Willebrand factor), FLT 1 (known as VEGFR receptor-1), CD 31 (known as PECAM) and Tie-2 (known as angiopoietin receptor), was similarly and highly expressed in both CB-EPCs (P3) and HUVECs (P3) (Supplementary Figure 1B). Besides, the translational expression patterns of KDR, VE-cad, FLT 1, CD 31 and Tie-2 from both CB-EPCs and HUVECs were similarly found by FACS analysis (Supplementary Figure 1C). The Immunocytochemistry staining using antibodies showed that strong fluorescence brightness

of vWF (green) and PECAM (red) was observed on the membrane and in the cytoplasm of both CB-EPCs and HUVECs, respectively (Supplementary Figure 1D). The functional analysis of CB-EPCs was further compared with HUVEC by tubule formation which is very critical for angiogenesis process and is considered as specific functional characteristics of endothelial and endothelial progenitor cells. When both CB-EPCs and HUVECs were cultured on matrigel, tubule-like structures were imitated within 6 hr after plating on matrigel,

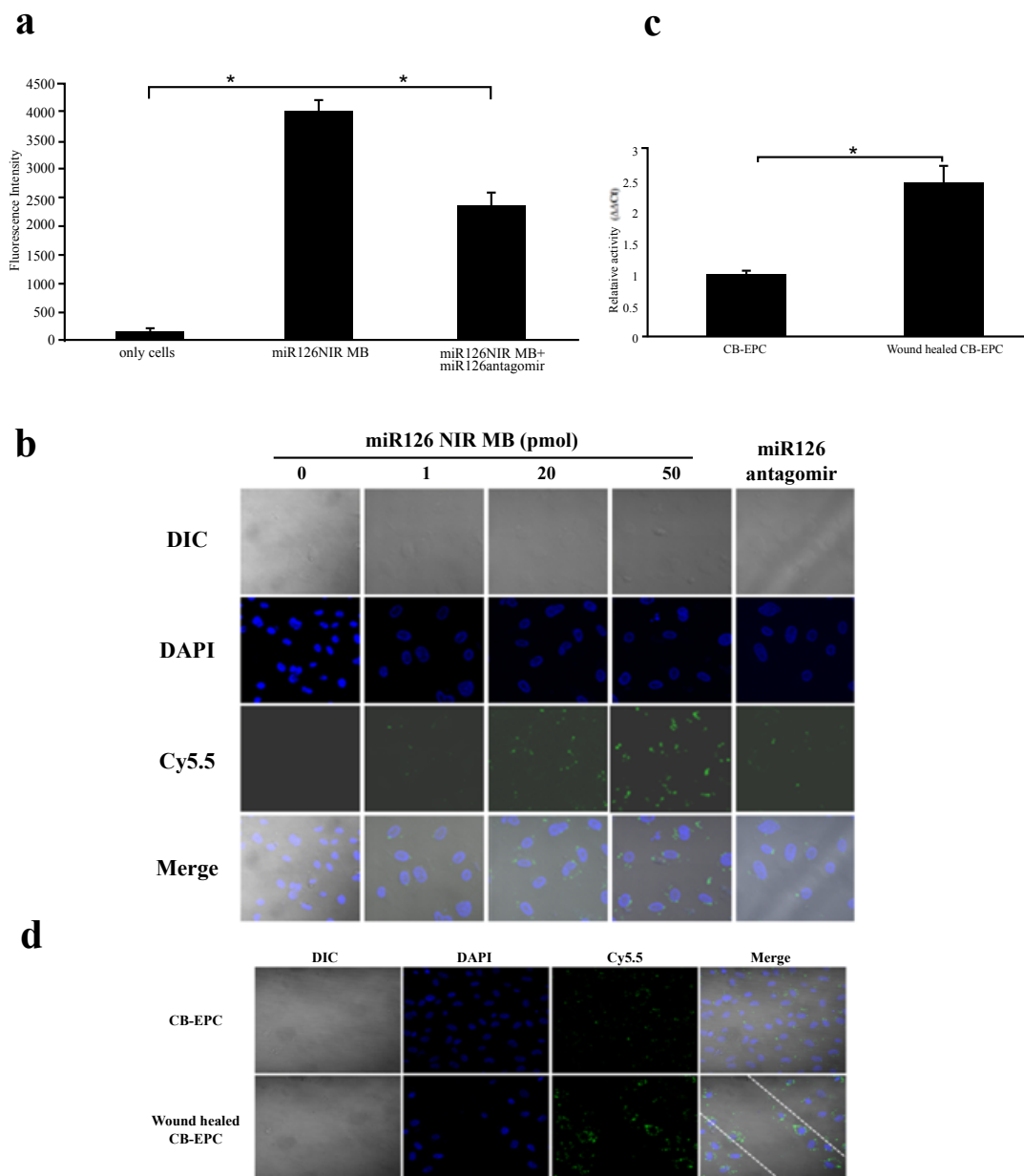


**Figure 3:** a) Fluorescence analysis of the miR126 NIR MB in CB-EPCs. The miR126 NIR MB (50 pmol) was transfected alone or with 100 pmol of miR126 antagomir into CB-EPCs. Cells only indicated the fluorescence intensity of CB-EPCs without the transfection of the miR126 NIR MB. Data were displayed as mean  $\pm$  standard error ( $*P < 0.05$ ). b) Confocal microscopy imaging (X800) of CB-EPCs transfected with the miR126 NIR MB. The miR126 NIR MB (0, 1, 20, and 50 pmol) was transfected alone or with 100 pmol of miR126 antagomir into CB-EPCs. All figures were merged with the 4', 6-diamidino-2-phenylindole (DAPI) image (nucleus staining, 460 nm) and cellular morphology. c) Real time PCR of CB-EPCs from the wound healing. Intact CB-EPCs was used as a control. Data were displayed as mean  $\pm$  standard error ( $*P < 0.05$ ). d) Confocal microscopy imaging (X800) of the miR126 NIR MB in CB-EPCs of the wound healing model. Dotted white lines highlighted the edges of a stripped region. Intact CB-EPC was used as a control. All figures were merged with the 4', 6-diamidino-2-phenylindole (DAPI) image (nucleus staining, 460 nm) and cellular morphology.

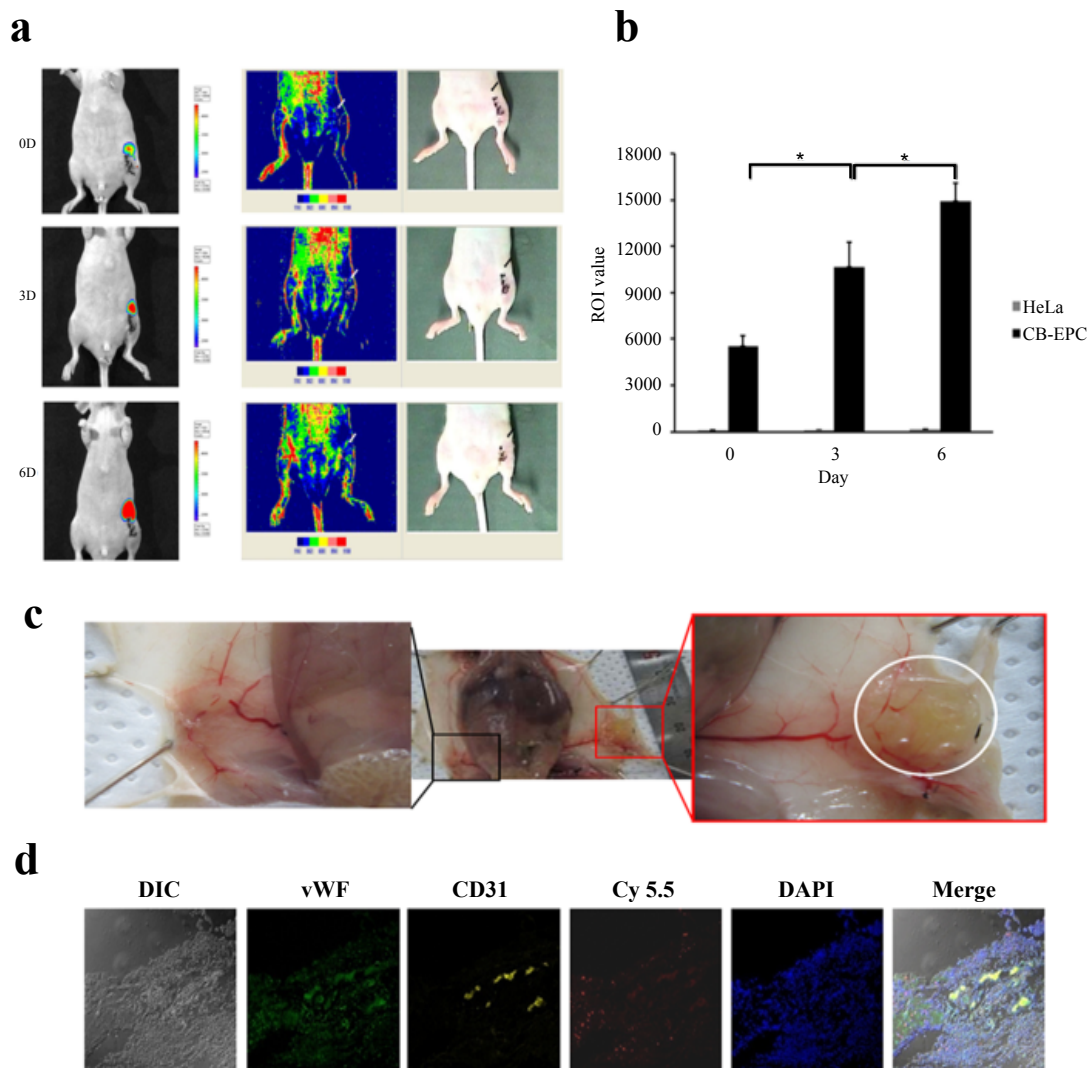


**Figure 4:** *In vivo* imaging of the miR126 NIR MB from the CB-EPCs-treated ischemia.

a) *In vivo* fluorescence imaging of the miR126 NIR MB (1<sup>st</sup> column), laser Doppler imaging (2<sup>nd</sup> column) and video image (3<sup>rd</sup> column) from the CB-EPCs-treated hind limb ischemia mouse for 6 days. The miR126 NIR MB transfected into  $2 \times 10^6$  of CB-EPCs was seeded into a matrigel then implanted into the unilateral hind limb ischemia mouse (indicated by a white (2<sup>nd</sup> column) or black (3<sup>rd</sup> column) arrow). b) ROI analysis of the *in vivo* fluorescence activity of the miR126 NIR MB from the 1<sup>st</sup> column of Figure 5A and Figure S1A. Data were displayed as mean  $\pm$  standard error ( $*P < 0.05$ ). c) Anatomy analysis of the CB-EPCs-treated hind limb ischemia 6 days after the implantation. The implanted region of the CB-EPCs-incorporated matrigel was magnified by a white circle. CB-EPCs in the matrigel formed vascular tubes that were connected to the host circulation. CB-EPCs were able to produce a dense network of blood vessels that were distributed uniformly throughout the matrigel. d) Double Immunohistochemistry staining of CD31 and vWF in the CB-EPC-treated hind limb ischemia. Confocal microscopy images (X400) of the slice sectioned from the CB-EPC-incorporated matrigels isolated from the CB-EPC-treated hind limb ischemia were conducted using CD31 (yellow) and vWF (green) antibodies. Blue fluorescence represented DAPI which stained the nucleus. Red fluorescence represented the miR126 NIR MB.

structurally well organized with more branches within 24 hr after plating, and were sustained 48 hr after plating (Supplementary 1E). These findings demonstrated, compared with HUVECs, that the isolated CB-EPCs possessed clear phenotypic and genotypic characteristics as endothelial progenitor cells, implying the potential that will be used for the neovascularization of EPC-treated cellular therapy of ischemia [37].

#### ***In vitro* imaging of mir126 expression in CB-EPCs using the mir126 biosensor**

To image endogenous expression of mir126 by the mir126 biosensor, the mir126 NIR MB was transfected into CB-EPCs. The quantitative fluorescence signals of the mir126 NIR MB in CB-EPCs was significantly increased due to the high expression of endogenous

mir126 in CB-EPCs which resulted in fluorescence recovery from the quenched the mir126 NIR MB (Figure 3A). The additional treatment of the mir126 antagomir into CB-EPCs significantly resulted in the decrease in fluorescence recovery of the mir126 NIR MB due to the hybridization of the mir126 antagomir with endogenous mir126 that blocked the hybridization of mature mir126 to the mir126 NIR MB and maintained the quenched status of the mir126 biosensor. Similarly, confocal microscopy imaging demonstrated, from the cytoplasm of CB-EPCs where mature miRNAs are generally expressed, that the NIR fluorescence recovery and brightness of the mir126 NIR MB were gradually increased in response to 0, 1, 20 and 50 pmol of the mir126 NIR MB due to the high expression of endogenous mir126, while the cytoplasmic fluorescence activity of the mir126 NIR MB from CB-EPCs

almost remained quiescent in the presence (100 pmol) of the mir126 antagomir (Figure 3B). To sense mir126 expression during angiogenesis, a wound healing migration assay was established by stripping away a region where CB-EPCs were grown to confluence. Real-time PCR showed that activity and expression of mir126 from CB-EPCs of the wound healing migration assay was significantly increased about 2.5-fold higher than intact CB-EPCs (Figure 3C). Confocal microscopy image demonstrated that cellular migration of CB-EPCs beyond the stripped area was monitored to heal the wound 24 hours after the excision (indicated by dotted lines) in the culture plate (Figure 3D). The transfection of the mir126 NIR MB into the wound healing model showed that NIR fluorescence brightness in the cytoplasm of CB-EPCs migrated into the stripped area was clearly visualized and relatively higher than that of CB-EPCs located behind the stripped region and intact CB-EPCs, due to the active angiogenesis of intact CB-EPCs near the stripped region which resulted in the more activated and increased expression of endogenous mir126 than gene expression of endogenous mir126 from intact CB-EPCs. These results showed a great sensitivity of the mir126 NIR MB to sense change of mir126 expression during angiogenesis of CB-EPCs.

### **In vivo imaging of CB-EPC-treated cellular therapy of ischemia using the mir126 NIR MB**

For *in vivo* biosensing of mir126 using the mir126 biosensor during EPC-treated cellular therapy of ischemia, the femoral artery only from the right hind limb of a mouse was first ligated. The mir126 NIR MB was transfected into  $2 \times 10^6$  of CB-EPCs or HeLa cells (used as a control). Since EPCs are well known to produce angiogenesis and vascularization in a matrigel *in vivo* (reference), CB-EPCs were further seeded into a matrigel. The cells-incorporated matrigels were then transplanted in the unilateral hind limb ischemia. From the CB-EPCs transplanted into the right hind limb, the NIR fluorescence signals of the mir126 NIR MB and limb perfusion by laser Doppler imaging were gradually increased for 6 days after hind limb surgery (Figure 4A). Interestingly, the NIR fluorescence signals by the IVIS system were much stronger than that by the laser Doppler imaging, implying that the mir126 NIR MB will be useful for early detection of CB-EPC-treated vascularization of ischemia. The *in vivo* fluorescence activities of the mir126 NIR MB from the CB-EPCs transplanted into the right hind limb, as determined by region of interest (ROI), was about 3-fold higher on day 6 than that on day 0 (Figure 4B). Although we could not evaluate the change in blood flow by the mean perfusion unit, blood vessel expansion from the CB-EPCs-incorporated scaffold was clearly observed at day 6 (Figure 4C). However, the control group implanted with HeLa cells into the right ischemic hind limb showed no significant fluorescence activity of the mir126 NIR MB (Figure 4B and Supplementary Figure 2A), no limb perfusion and no blood vessel expansion (Supplementary Figure 2B). To evaluate *in vivo* fluorescence imaging of mir126-involved angiogenesis from CB-EPC treated hind limb ischemia, the CB-EPC- and HeLa cells-incorporated matrigels were isolated from the right hind limb of the ischemia mouse at 6-day-postinjection. From the tissue section of the CB-EPC-incorporated matrigels, cellular morphology showed well connection of a mesh-like network between cells to form vascular tubes while this observation was not found in the HeLa cells-incorporated matrigels (Figure 4D) (Supplementary Figure 2C). Besides, immunohistochemical analysis using antibodies of vWF and CD31 confirmed angiogenesis progression in the CB-EPC-treated hind limb ischemia mouse. It is noted that high expression of CD31 which is important for tube formation may provide the evidence of blood circulation (reference). Additionally, H&E staining showed rbc-filled lumens from the tissue section of the EPC-incorporated matrigel but

not from HeLa cell-incorporated matrigel (Supplementary Figure 3). Rbc-filled lumen is one of critical signs for the presence of functional microvascular vessels (reference). The fluorescence brightness of the mir126 NIR MB was clearly visualized from the CB-EPC-treated hind limb ischemia mouse. However, no clear evidence of angiogenesis and no fluorescence activity of the mir126 NIR MB were found in the isolated HeLa cells-incorporated matrigels. The co localization of fluorescence signals among vWF, CD31 and the mir126 NIR MB from the isolated CB-EPC-incorporated matrigels provided the evidence that *in vivo* imaging signals of the mir126 NIR MB were acquired due to the cellular therapy of the ischemia by the mir126 regulating angiogenesis of the implanted CB-EPCs.

### **Discussion**

Molecular imaging, which integrates molecular biology with *in vivo* imaging, can conduct the non-invasive monitoring of the cellular function and the follow-up molecular function in living organisms without sacrificing the animals. Most of current *in vivo* imaging methods including X-ray, CT and MRI for angiogenesis and vascularization have displayed cellular morphology including blood vessels instead of providing imaging information about gene expression related to angiogenesis and vascularization, which is frequently difficult for the accurate and early diagnosis for malignancy or new growth of blood vessels. The limitation of the tissue or cellular morphology-based imaging methods can be overcome by molecular probes known as biomarkers which help image dynamic change of molecular targets of interest that strongly and specifically express and precede change of cellular phenotype.

Mir126 known to be induced by VEGF is a good candidate biomarker for imaging blood vessel formation which is expressed specifically and highly during the process of angiogenesis and vascularization of endothelial cells. In this study, the mir126 NIR MB was successfully developed to sense endogenous mir126 expression and visualized EPC-treated cellular therapy of the hind limb ischemia. The high expression of mir126 from CB-EPCs was specifically bound to the complementary oligonucleotide sequences in the stem loop of the mir126 NIR MB and resulted in the separation of the Cy5.5 and BHQ2, producing fluorescence recovery. This great sensitivity of sensing mir126 by the mir126 NIR MB clearly visualized the difference in mir126 expression CB-EPCs before and after the activation of angiogenesis induced by the wound healing model. Moreover, from the *in vivo* imaging of EPC-treated cellular therapy of the hind limb ischemia, fluorescence signals of the mir126 NIR MB from CB-EPCs was much stronger than the signals of laser Doppler imaging, demonstrating that the mir126 sensor will provide a useful imaging probe for early diagnosis of cellular therapy of ischemia. Moreover, the fluorescence characteristics of NIR from the mir126 NIR MB showed a significantly low background of *in vivo* imaging from CB-EPCs-treated cellular therapy of ischemia for 6 days due to the high signal-to-background ratio of Cy5.5. Besides, similar with other reports (reference), our CB-EPCs which were incorporated into the matrigel demonstrated high expression of CD31 and lumen formation *in vivo*. These results indicate that the matrigel may help cell elongation, migration and invasion and cell-cell association to eventually form tube network structure for blood circulation at the ligation site of the femoral artery. Although we did not compare therapeutic effect of CB-EPC-treated hind limb ischemia with or without the matrigel, the matrigel as a carrier of CB-EPC will be useful for future clinical application.

Our previously developed miRNA imaging systems using a bioluminescent reporter gene and a fluorescence molecular beacon

are a signal-off system and a signal-on system with high background in response of miRNA expression, respectively [29,35]. The signal-off system had the limitation of differentiating decreased signals from cellular loss or miRNA expression. The signal-on miRNA imaging system had a high fluorescent background of *in vivo* imaging with rhodamine, 6-FAM and Texas Red fluorescence dyes. Therefore, the mir126 NIR MB overcomes both limitations by providing a signal-on imaging intensity in response to mir126 expression and low fluorescence background of *in vivo* imaging. Since miRNA have been linked to various cellular processes including proliferation, differentiation and apoptosis and diseases including cancer, diabetes, and neurological [15,38-39], the miRNA NIR MB will provide non-invasively sensitive imaging information about cellular developments, diagnosis of disease and cellular therapy related to the miRNA function.

## Conclusion

We have successfully developed a NIR-based mir126 MB biosensor of imaging mir126-related angiogenesis during EPC-treated cellular therapy of ischemia. The miRNA NIR MB can be used for *in vitro* and *in vivo* imaging of various miRNA, which can sensitively monitor real-time visualization of miRNA-involved cellular developments and disease treatments using stem cells through repetitive imaging of the same animals.

## Acknowledgments

This work was supported by the Bio and Medical Technology Development Program of the National Research Foundation (NRF) funded by the Korean government (MEST) (No. 2011-0019270) and a grant of the Korea Healthcare technology R&D Project, Ministry of Health and Welfare (A120254).

## References

- Asahara T, Murohara T, Sullivan A, Silver M, van der Zee R, et al. (1997) Isolation of putative progenitor endothelial cells for angiogenesis. *Science* 275: 964-967.
- Masuda H, Kalka C, Asahara T (2000) Endothelial progenitor cells for regeneration. *Hum Cell* 13: 153-160.
- Hur J, Yoon CH, Kim HS, Choi JH, Kang HJ, et al. (2004) Characterization of two types of endothelial progenitor cells and their different contributions to neovascularization. *Arterioscler Thromb Vasc Biol* 24: 288-293.
- Haylock DN, Nilsson SK (2007) Expansion of umbilical cord blood for clinical transplantation. *Curr Stem Cell Res Ther* 2: 324-335.
- Copeland N, Harris D, Gaballa MA (2009) Human umbilical cord blood stem cells, myocardial infarction and stroke. *Clin Med* 9: 342-345.
- Lin SZ (2011) Advances in translational stem cell research and therapies. *Cell Transplant* 20: 1-3.
- Zeng Y, Wagner EJ, Cullen BR (2002) Both natural and designed micro RNAs can inhibit the expression of cognate mRNAs when expressed in human cells. *Mol Cell* 9: 1327-1333.
- Eulalio A, Huntzinger E, Izaurralde E (2008) Getting to the root of miRNA-mediated gene silencing. *Cell* 132: 9-14.
- Iorio MV, Croce CM (2009) MicroRNAs in cancer: small molecules with a huge impact. *J Clin Oncol* 27: 5848-5856.
- Zeng Y, Yi R, Cullen BR (2003) MicroRNAs and small interfering RNAs can inhibit mRNA expression by similar mechanisms. *Proc Natl Acad Sci U S A* 100: 9779-9784.
- Brennecke J, Hipfner DR, Stark A, Russell RB, Cohen SM (2003) Bantam encodes a developmentally regulated microRNA that controls cell proliferation and regulates the proapoptotic gene *hid* in *Drosophila*. *Cell* 113: 25-36.
- Xu P, Vernooij SY, Guo M, Hay BA (2003) The *Drosophila* microRNA *Mir-14* suppresses cell death and is required for normal fat metabolism. *Curr Biol* 13: 790-795.
- Dostie J, Mourelatos Z, Yang M, Sharma A, Dreyfuss G (2003) Numerous microRNPs in neuronal cells containing novel microRNAs. *RNA* 9: 180-186.
- Zamore PD, Haley B (2005) Ribo-gnome: the big world of small RNAs. *Science* 309: 1519-1524.
- Croce CM, Calin GA (2005) MiRNAs, cancer, and stem cell division. *Cell* 122: 6-7.
- Sullivan CS, Ganem D (2005) MicroRNAs and viral infection. *Mol Cell* 20: 3-7.
- Weiler J, Hunziker J, Hall J (2006) Anti-miRNA oligonucleotides (AMOs): ammunition to target miRNAs implicated in human disease?. *Gene Ther* 13: 496-502.
- Kloosterman WP, Plasterk RH (2006) The diverse functions of microRNAs in animal development and disease. *Dev Cell* 11: 441-450.
- Dews M, Homayouni A, Yu D, Murphy D, Seignani C, et al. (2006) Augmentation of tumor angiogenesis by a Myc-activated microRNA cluster. *Nat Genet* 38: 1060-1065.
- Poliseno L, Tuccoli A, Mariani L, Evangelista M, Citti L, et al. (2006) MicroRNAs modulate the angiogenic properties of HUVECs. *Blood* 108: 3068-3071.
- Kuehbach A, Urbich C, Zeiher AM, Dimmeler S (2007) Role of Dicer and Drosha for endothelial microRNA expression and angiogenesis. *Circ Res* 101: 59-68.
- Fish JE, Santoro MM, Morton SU, Yu S, Yeh RF, et al. (2008) MiR-126 regulates angiogenic signaling and vascular integrity. *Dev Cell* 15: 272-284.
- Bonauer A, Carmona G, Iwasaki M, Mione M, Koyanagi M, et al. (2009) MicroRNA-92a controls angiogenesis and functional recovery of ischemic tissues in mice. *Science* 324: 1710-1713.
- Cordes KR, Sheehy NT, White MP, Berry EC, Morton SU, et al. (2009) miR-145 and miR-143 regulate smooth muscle cell fate and plasticity. *Nature* 460: 705-710.
- Wang S, Aurora AB, Johnson BA, Qi X, McAnally J, et al. (2008) The endothelial-specific microRNA miR-126 governs vascular integrity and angiogenesis. *Dev Cell* 15: 261-71.
- Yang LT, Nichols JT, Yao C, Manilay JO, Robey EA, et al. (2005) Fringe glycosyltransferases differentially modulate Notch1 proteolysis induced by Delta1 and Jagged1. *Mol Biol Cell* 16: 927-942.
- Kuehbach A, Urbich C, Dimmeler S (2008) Targeting microRNA expression to regulate angiogenesis. *Trends Pharmacol Sci* 29: 12-15.
- Joshi BP, Wang TD (2010) Exogenous Molecular Probes for Targeted Imaging in Cancer: Focus on Multi-modal Imaging. *Cancers (Basel)* 2: 1251-1287.
- Lee JY, Kim S, Hwang do W, Jeong JM, Chung JK, et al. (2008) Development of a dual-luciferase reporter system for in vivo visualization of MicroRNA biogenesis and posttranscriptional regulation. *J Nucl Med* 49: 285-294.
- Krichevsky AM, King KS, Donahue CP, Khrapko K, Kosik KS (2003) A microRNA array reveals extensive regulation of microRNAs during brain development. *RNA* 9: 1274-1281.
- Ko HY, Lee DS, Kim S (2009) Noninvasive imaging of microRNA124a-mediated repression of the chromosome 14 ORF 24 gene during neurogenesis. *FEBS J* 276: 4854-4865.
- Ko MH, Kim S, Hwang do W, Ko HY, Kim YH, et al. (2008) Bioimaging of the unbalanced expression of microRNA9 and microRNA9\* during the neuronal differentiation of P19 cells. *FEBS J* 275: 2605-2616.
- Hwang do W, Song IC, Lee DS, Kim S (2010) Smart magnetic fluorescent nanoparticle imaging probes to monitor microRNAs. *Small* 6: 81-88.
- Kang WJ, Cho YL, Chae JR, Lee JD, Choi KJ, et al. (2011) Molecular beacon-based bioimaging of multiple microRNAs during myogenesis. *Biomaterials* 32: 1915-1922.
- Kang WJ, Cho YL, Chae JR, Lee JD, Ali BA, et al. (2012) Dual optical biosensors for imaging microRNA-1 during myogenesis. *Biomaterials* 33: 6430-6437.
- Harris TA, Yamakuchi M, Kondo M, Oettgen P, Lowenstein CJ (2010) Ets-1 and Ets-2 regulate the expression of microRNA-126 in endothelial cells. *Arterioscler Thromb Vasc Biol* 30: 1990-1997.
- Asahara T, Kawamoto A (2004) Endothelial progenitor cells for postnatal vasculogenesis. *Am J Physiol Cell Physiol* 287: 572-579.
- Ambros V (2004) The functions of animal microRNAs. *Nature* 431: 350-355.
- Miska EA, Alvarez-Saavedra E, Townsend M, Yoshii A, Sestan N, et al. (2004) Microarray analysis of microRNA expression in the developing mammalian brain. *Genome Biol* 5: 68.